The Ohio State University

GrowFlesh:

The Lightweight, Customizable, Epithelial Tissue Simulator

Author:
Melvyn Ian Drag
B.A. Mathematics

Advisors:
Dr. Marcos Manuel Sotomayor
Dr. Edward Overman

Presented in partial fulfillment of the requirements for the degree
Master of Mathematical Sciences
in the Graduate School of The Ohio State University

April 5, 2015

Abstract

Epithelial tissue is introduced, current models of epithelial development are described, and then a new implementation of a long existing model is presented. The code for the model is thoroughly examined and the algorithms and data structures underlying it are presented. Some topological insights are made about the nature of epithelial tissue, and some discussion of which numerical methods are used is made.

a mis escuincles Alfie and Andy

Acknowledgements

Vita

Contents

List of Figures

Chapter 1

Why Study Epithelial Tissue?

Epithelial tissue covers the interior and exterior surfaces of our bodies. Skin, the lining of the esophogas and intestines, the urethra, the lining of the lungs and all of the bronchioles in the lungs are all made up of epithelial tissue. In this way, we can think of epithelial tissue as being the envelope in which our contents are packaged [**?**]; epithelial tissue is our interface with the outside world. This definition of course extends to all animals and even to plant life, as plants have a single layered epithelial tissue that covers their exposed leaves, flowers, roots, and stems.

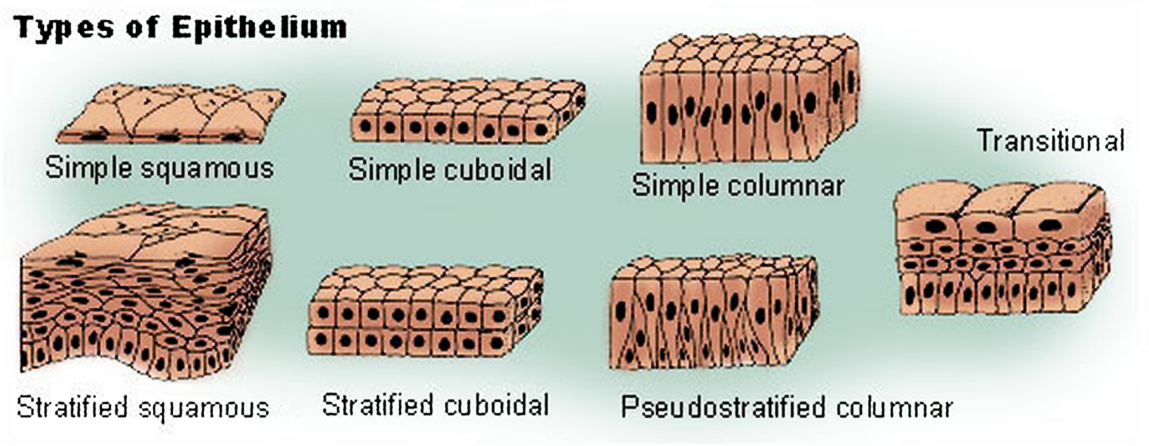

Figure 1.1: The Types of Epithelial Tissue

Botanical epithelia are rather simple and homogeneous - a single layer of cells covering exposed surfaces. As Figure **??** shows, however, there are many types of epithelial tissue in animals which vary in the number of layers they include, how the cells are shaped, and how tall the cells are. Each of these types of cells are found in a different region of the body where they perform a specific function. For example, the simple squamous epithelium is no more than one layer of cells thick, and the cells are all very flat, much flatter than they are wide. These cells are therefore well suited to allow diffussion across themselves. As such, simple squamous tissue is found in the walls of blood vessels, and in the alveoli in the lungs, where the diffusion of oxygen occurs. On the other hand, columnar cells are much taller than they are wide, and are thus well suited to absorption. These cells are found in the intestines where they absorb nutrients from passing food. Stratified squamous epithelia are several layers thick line the esophogas and mouth and serve to protect against abraision.

What all of these tissues have in common, however, is how amenable they are to computational modeling. The simplest case is that of simple epithelia, which typically have near-uniform height, and very little difference in appearance between their apical and basal faces. This means that the cells can easily be approximated by two dimensional meshes,

since the top and bottom of the cells move in tandem and the surface where two cells touch can be approximated by a line. Slightly more difficult is the modeling of stratified tissue. In this case, the tissue develops in three dimensions, since underlying cells affect the cells on top of them. These cannot be modeled in two dimensions, but can be modeled by a solid composed of three dimensional polytopes. The theory behind these models is well developed, but the techincal details of implementing such a model has made it so that very exist, and are often quite limited [1].

To give you an idea of what current epithelial tissue simulators have produced, I am putting some images from recent papers.

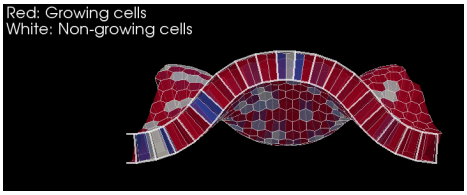

(a) Simple Squamous Tissue Bending in 3D[**?**]

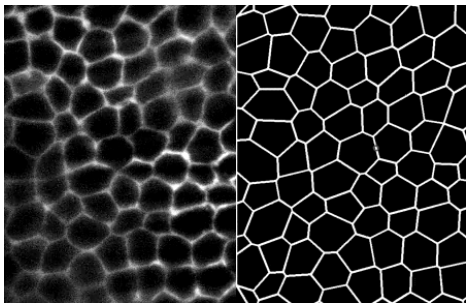

(b) Comparison of Living Tissue and Simulation[**?**]

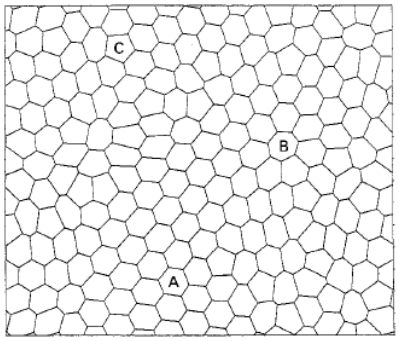

(c) Equilibrium Mesh[**?**]

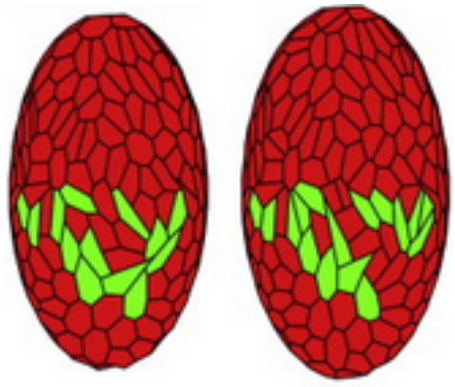

(d) Equilibrium Mesh on a 3d Surface [**?**]

Figure 1.2: Some existing models of epithelial tissue.

So, the question still remains: "Why Study Epithelial Tissue?". The study of biological tissues has intrinsic value, much as mapping constellations or studying the properties of natural numbers. Beyond its inherent worth, current research in epithelial tissue is producing great results in the field of epithelial tissue morphogenisis and diversifictation as well as wound healing. The Honda-Nagai model which we will discuss in great detail in this paper successfully reproduced the dynamics of the healing of wounds to cats' corneas[**?**]. This model has also been able to reproduce all of the essential dynamics of epithelial tissue [**?**]. So, in conclusion, we *should* be modeling epithelial tissue computationally because it is easy to do, effective, an the community is currently very active and passionate about the field.

[1] Even a leading epithelial tissue simulator, Chaste, still does not have stable 3D modeling capabilities

Chapter 2

Overview of the Model

The world was so recent that many things still lacked names,
and to mention them one had to point with a finger.
- Gabriel Garcia Marquez

2.1 Introduction

A two dimensional **vertex dynamics model** of epithelial tissue is made up of vertices and edges. A cell is represented as a convex hull made up of cells and vertices. This model presupposes that the movement of cells in epithelial tissue can be approximated by the movement of the vertices which make up the cell. Some force is hypothesized to be the guiding force between epithelial cell movement, and this force is applied to all of the vertices in the mesh of cells, producing some final state of the tissue. The three dimensional model is an extension of the two-dimensional model, but the mesh comes to include not only vertices and edges, but also cell faces.

Epithelial vertex dynamics has been a lively field of research since the 1970s because of several heartening results in the field. Some researchers have had success modelling the morphogenesis of *Drosophila* wing growth, whereas other researchers have successfully reproduced the dynamics of corneal wound healing. Unfortunately, these results have not come from one standard force, but from a variety of different hypothesized forces.

As an example of the different approaches to force modelling, let us consider the Weliky-Oster and Honda-Nagai forces. The Weliky-Oster model specifies explicit forces which act act upon the vertices due to a tension associated with boundary lengths. In two dimensions this constributes two tensions from each edge in a cell surrounding a vertex. The model also includes a cortical pressure due to the osmotic pressure inside a cell, which tends to push a vertex away from the interior. The Honda-Nagai Model (which I have recreated) takes a much different approach and instead specifies a potential energy function for the tissue. In this model the cells move passively as they attempt to minimize the potential energy of the tissue[**?**].

While both of these models successfully reproduce the topological and geometric properties of epithelial tissue, I have chosen to focus my efforts on the Nagai-Honda model. So, let us look at the model in some depth.

2.2 The Nagai-Honda Model

2.2.1 How the Vertices Move

A very basic result from physics is the relationship between force and potential energy, and this is one of the building blocks of the Nagai-Honda Model. Given a force vector F and scalars U, for potential energy and W for work, we can derive the relation:

Figure 2.1: The Giant's Causeway

$$\vec{F} = (F_x, F_y, F_z) \tag{2.1}$$

$$W = -\Delta U(\vec{x}) = \int_{x_0}^{x} F_x dx + \int_{y_0}^{y} F_y dy + \int_{z_0}^{z} F_z dz \tag{2.2}$$

$$\nabla(-\Delta U(\vec{x}) = \nabla\left(\int_{x_0}^{x} F_x dx + \int_{y_0}^{y} F_y dy + \int_{z_0}^{z} F_z dz \right) \tag{2.3}$$

$$-\nabla U(\vec{x}) = \vec{F} \tag{2.4}$$

The second building block of the Nagai-Honda Model is the equation of motion. In 1989, K. Kawaski showed that the dynamics of grain growth can be reduced to a first order system given by:

$$\eta \frac{dr_i}{dt} = F_i \tag{2.5}$$

where F_i denotes the force applied to vertex i and the left hand side is the velocity of the vertex multiplied by a positive drag coefficient, η[**?**].

A very important paper in the field of natural cellular structures, of which the study of epithelial tissue is a small subset, is *Soap, Cells, and Statistics*. In this paper, leading researchers in the field argue that there must be some natural mechanism underlying the development of epithelial tissue, columnar basalt formations, soap froths, grin growths, and other cellular structures, as they exhibit a great deal of similarity. For example, consider the images of epithelial tissue presented throughout this paper next to the image of The Giant's Causeway in Northern Ireland. Some differences include the exact distribution of cell shapes, the presence of chemicals in biological tissues versus the absence of growth inducing chemicals in geological structures, and the active migration of biological cells versus the entirely passive movement of soap froths; still, the equilibrium patterns of these diverse structures leads one to believe that there must be some underlying principle. The Honda-Nagai model builds upon this idea and borrows ideas from the field of grain growth.

Putting these building blocks together, we have a force acting on the vertices in the mesh, and an equation of motion which explains how the vertices move. Now all that is needed is a free energy function from which to derive our force (and this force should be similar to the force found in other cellular structures). The free energy function which

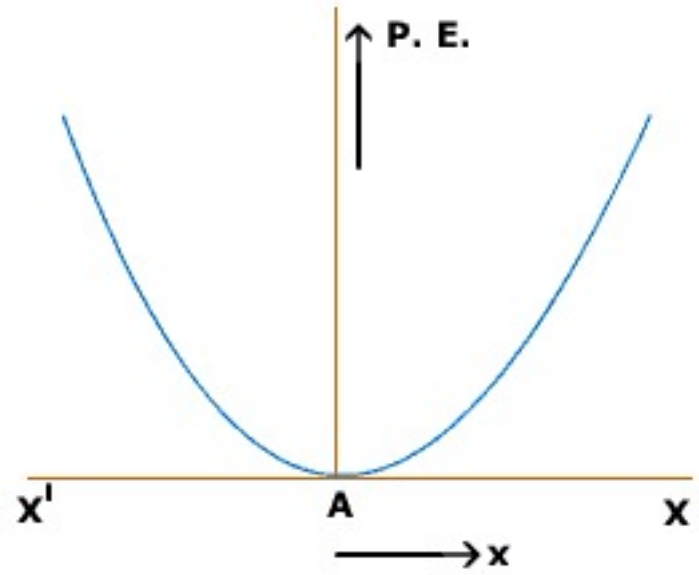

Figure 2.2: Potential Energy as a Function of Distance from Equilibrium.

provides the applied force was taken in part from the grain growth model, which asserts that grains want to achieve a target volume and perimeter via some still unknown mechanism. As previously mentioned, biological cellls have idiosynchratic mechanisms working on them as well. As such, the model was extended to include a purely biological factor, *differential adhesion*. It is well known that cells have a proclivity to attach more tightly to certain cells than to others due to the presence of certain cadherin proteins in the membranes of the cells. This tendency is called differential adhesion.

The first two energy terms assume that the cell is elastic, and that the cell wants to return to a target shape. Therefore, the first two energy terms are of the elastic potential form:

$$C(x - x_0)^2 \tag{2.6}$$

where x is some physical quantity, and C is some constant. The plot of this energy is therefore a parabola with a minimum at $x = x_0$ (A replaces x_0 in Figure **??**) and the farther x is from x_0, the more potential energy there will be in the cell. The last energy term is an adhesion energy, which is proportional to the amount of interfacial surface area between a cell and its neighbor. Here are the three energy terms:

1. The deformation energy term

$$U_D = \lambda(A - A_0)^2 \tag{2.7}$$

   where A_0 is a target area for a cell, and lambda is some positive constant.

2. The membrane surface energy

$$U_S = \beta(C - C_0)^2 \tag{2.8}$$

   where C is the cell perimiter, and C_0 is a target perimeter.

3. The cell-cell adhesion energy

$$U_A = \sum_{j=1}^{n} \gamma_j d_j \tag{2.9}$$

where n is the number of vertices in the cell, γ is some constant for the boundary in question between one cell and another, and d is the distance between one vertex and the next in a counter clockwise fashion. Note that in two dimensins the boundary is a distance d, but in three dimensions it would have to be the area of a cell face. Also take note of the fact that the gamma term could be implemented in various ways. I have chosen to assign a "stickiness" to each cell, and then the gamma term is calculated as the average of the stickiness of the two cells.

As seen in [**?**], this force on each vertex i is given by the negative gradient of the potential:

$$F_i = -\sum_{l \in N_i} (2\lambda(A_l - A_{0_l})\nabla_i A_l + 2\beta(C_l - C_{0_l})(\nabla_i d_{l,I_l-1} + \nabla_i d_{l,I_l}) + \gamma_{l,I_l-1}\nabla_i d_{l,I_l-1} + \gamma_{l,I_l}\nabla_i d_{l,I_l} \tag{2.10}$$

where l is the lth cell containing vertex i, given a counter clockwise orientation. I_l is the local index of node i in element l.

The way to derive this force is not described in much of the literature, and only is partially described in [**?**]. I will explain the force in some detail here.

The area of a cell is given by Gauss's Shoelace Formula:

$$A = \frac{1}{2}\Big|\sum_{i=1}^{N}\Big(x_i y_{i+1} - x_{i+1} y_i\Big)\Big| \tag{2.11}$$

where N+1 = 1. Therefore, the gradient is given by:

$$\nabla_i A_l = \frac{1}{2}\Big\langle y^l_{I+1} - y^l_{I-1},\ \ x^l_{I-1} - x^l_{I+1}\Big\rangle \tag{2.12}$$

where the superscrpits l denote that x, y are in cell l. The subscripts are local indices in the cell l, and the orientation of vertices is counterclockwise. The circumference is given by:

$$C = \sum_{j=1}^{N} d_j = \sum_{j=1}^{N} \sqrt{(x_{j+1} - x_j)^2 + (y_{j+1} - y_j)^2} \tag{2.13}$$

Therefore

$$\nabla_i C = \nabla_i d_{i-1} + \nabla_i d_i \tag{2.14}$$

and

$$\nabla_i d_{l,j} = \frac{1}{d_{l,j}}\Big\langle x_{j+1} - x_j,\ \ y_{j+1} - y_j\Big\rangle \tag{2.15}$$

Substituting the above values into the equation:

$$-\nabla_i U = -\nabla_i (U_D + U_S + U_A) = F_i \tag{2.16}$$

gives the force described above.

2.2.2 Academic Dishonesty, or Obvious Modeling?

I am not at the point yet in my understanding of the physics of epithelial tissue to comment upon whether this model ought to be intuitively obvious to the physicist, or whether it is a carefully chosen model which has discarded many extraneous possibilities. A recent article [**?**] gives the equation for the potential in the mesh as:

$$E_i = \sum_{\alpha} \frac{K}{2}(A_\alpha - A_\alpha^0)^2 + \sum_{i,j} \Lambda_{ij} l_{ij} + \sum_{\alpha} \frac{\Gamma}{2} L_\alpha^2 \tag{2.17}$$

Where i denotes vertex i, α denotes a cell of which i is on the border, the A and A_0 terms denote area and target area, and the l_{ij} denotes the length of the boundaries on which i lies, and the L denotes the perimeter. The H. Honda or T. Nagai are not cited in the bibliography to this paper by several well known and respected scientists, so either this model is so obviously adecuate that it isn't necessary to cite the original author, or this is a case of academic dishonesty.

2.2.3 Topological Changes to the Mesh

There is emprirical evidence that nearly all vertices in a sheet of epithelial tissue have degree three. Since the coordination number of the almost all vertices is three, this has led many modelers to consider what sort of topological changes can occur in mesh of these types of cells without changing the connectivity. As it turns out, there are three changes which can occur. The first is called a T1 swap and in illustrated in Figure **??**. This is also called a "neighbor exchanging swap" because, as you can see, two cells which were adjacent cease to be neighbors and two cells that weren't adjacent become neighbors. The T1 swap occurs when two vertices become critically close to each other, and instead of allowing the force to drive the vertices into each other we rotate their edge by 90 degree. In nature this sould correspond to two vertices getting very close, colliding, and then flattening out into an edge. Our model performs this action discretly as a simplifying measure, however, because otherwise for a moment a vertex would have degree four, and this would be difficult to handle with out a very complex data structure. The second topological change is the T2 swap, which is also known as the "cell removal swap." This occurs when a triangular cell becomes too small and is deleted and replaced by a single vertex. The last swap is cell division, occasionally referred to as the T3 swap.

Cell division was not a part of the original Honda-Nagai Model, but it is now a very hot topic in computational tissue morphogenesis; it deserves mention. The challenge with implementing the T3 swap is that there are infinitely (within the bounds of floating point arithmetic) many choices about where to divide a cell, and there are several competing opinions (though no unanimouslly accepted theory) about how the dvision is oriented. Some cells divide along their longer axis, which is known as the 'Hertwig's Long Axis Rule', but global tissue stress and local cell geometry are also thought to affect the orientation of cell division [**?**][**?**]. The computational implementation of T3 swap is trivial, as the swap occurs by placing two new vertices in the interior of opposite edges and then connecting them by a new edge. The trouble is that it is not clear which edges ought to have vertices implanted, or where to insert these vertices, and the choice of where to divide a cell in a proliferating tissue can have profound effects upon the geometric appearance of a tissue [**?**]. There will be more discussion of cell division in the section of the paper dealing with the technical details of the implementation of *Epithelium*.

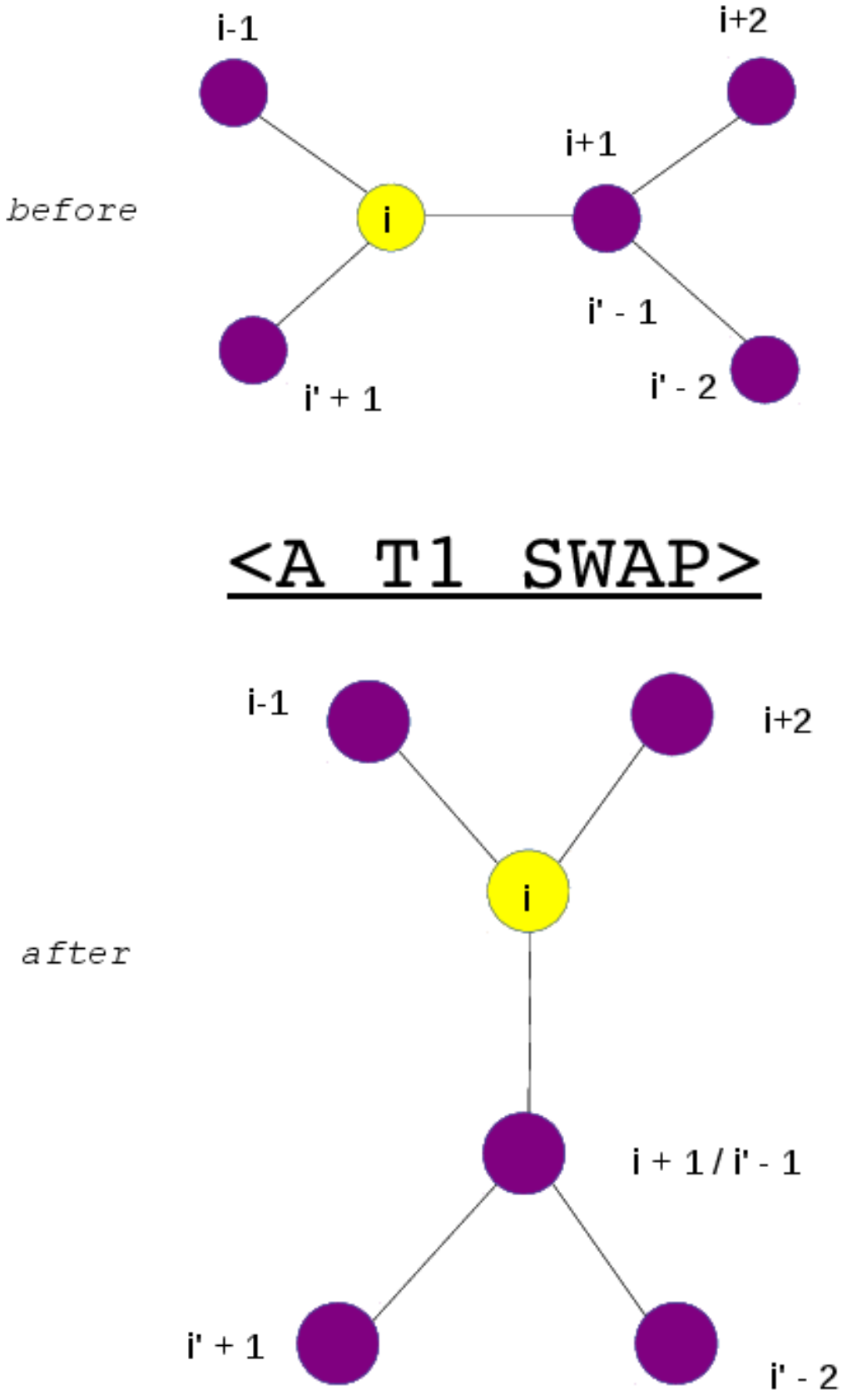

Figure 2.3: A T1 Swap

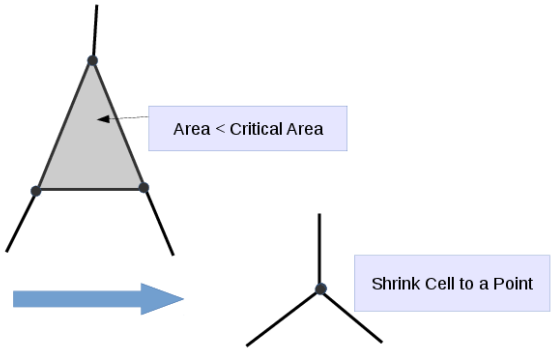

Figure 2.4: A T2 Swap

2.2.4 Quality, Not Quantity

The equations in this model are dimensionless. I will not undertake a discussion of how to derive the dimensionless model from the dimensional model, but for the curious reader this is all laid out in [**?**]. Typically, one would not choose the values of the parameters α, β and *gamma*, but would instead have some dimensional biological data and go through the necessary conversion steps to convert these parameters to the simpler ones. Interestingly, in vertex dynamics literature I have read and cited in the bibliography, the only clearly stated parameters appear in [**?**], and these are said to be taken from several papers which the authors (though I myself did not find these values explicity stated).

There is little difference between equilibrium states in the Nagai-Honda model, as can be seen in the section of this paper dealing with the output of the code. Still, it has been shown that different parameter values coupled with other mesh changing operations (such as oriented cell division) can cause drastically different types of morphogenesis [**?**]. For example, drosophila wings, with their highly oriented divisions, have been shown to contain approximately 80% hexagonal cells whereas cucumber epidermis contains approximately 47% hexagons [**?**]. While all epithelial tissue has a strong tendency towards achieving an equilibrium dominated by hexagons, the width of the distribution of cell shapes differs by cellular structure and, hence, by parameter choices [**?**].

For those interested I have included in this paper charts which display the equilibrium meshes for different parameter values, along with a graph of the equilibrium distributions of cell sizes. These tables are found in chapter TITLE OF CHAPTER HERE. What you will see in the charts is that my implementation of the Honda-Nagai Model reproduces the results of the authors' original paper in that given a wide variety of parameterizations the mesh tends towards six sided cells. Here is one graphic from [**?**] in which they illustrate the distribution of cell shapes as a function of time.

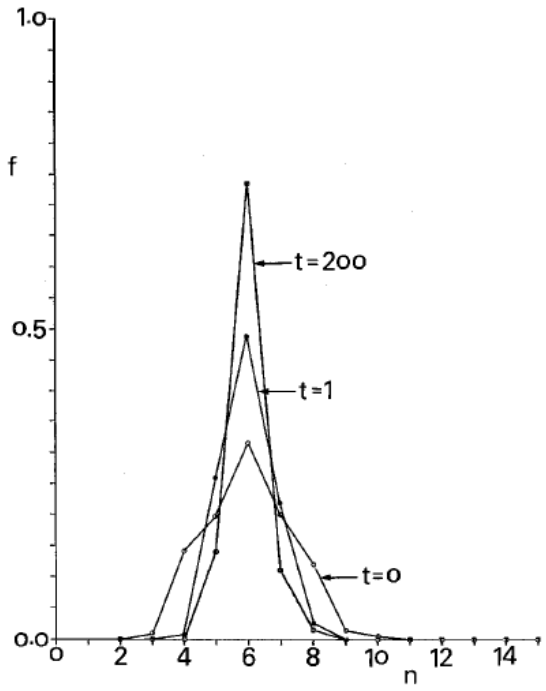

Figure 2.5: The Distribution of Cell Shapes As a Function of Time [**?**]

Chapter 3

Further Remarks About Epithelial Tissue and the Honda-Nagai Model

3.1 The Euler Characeteristic and Its Implications

In this section I will expand upon some observations made in [**?**]. **Euler's Formula** is an equation which relates the number of edges, faces, and vertices in a graph or polyhedron. An invariant χ relates the faces, edges, and vertices as follows:

$$\chi = V - F + E \tag{3.1}$$

The invariant depends upon the graph or polyhedron in question. We will ignore the exact value of χ and comfort ourselves with the fact that it is a constant. The majority or current vertex dynamics models assume that vertices will have a coordination number of 3, and are based upon empirical results from biology. While there are certain models which consider *rosettes*, for now we will assume that all vertices connect to exactly three other vertices. Then we notice that all edges have two vertices, and that all vertices are connected to three edges. Inititally, our intuition tells us that there should be three times as many edges as vertices, which leads us to the incorrect:

$$3V = E \tag{3.2}$$

But then we notice that if we consider all of the vertices in the mesh, we count each edge twice, so we divide the conjectured number of edges by two and then simplify to get:

$$3V = 2E \tag{3.3}$$

Similarly, if we consider how to relate the number of edges to the faces in the mesh, we conjecture that the number of edges in equal to the number of cells with 3 sides plus the number of cells with 4 sides plus the number of cells with 5 sides plus . . . each multiplied by the number of edges per cell. THis gives us:

$$\sum_{k=3}^{N} kF_k = E \tag{3.4}$$

Where N is the highest number of edges encountered by any cell in the mesh. But in this way we have again counted all of the edges twice, so the true number of edges must be the summation above divided by 2. We simplify the equation to :

$$\sum_{k=3}^{N} kF_k = 2E \tag{3.5}$$

Now, we are able to reduce Euler's Forula to one variable using the relationships given above.

$$V - F + E = \chi \tag{3.6}$$

$$\frac{2E}{3} - F + E = \chi \tag{3.7}$$

$$\frac{5E}{3} - F = \chi \tag{3.8}$$

$$\frac{\sum_{k=3}^{N} kF_k}{6} - F = \chi \tag{3.9}$$

$$(\frac{\sum_{k=3}^{N} kF_k}{F} - 6)F = 6\chi \tag{3.10}$$

Biological cells are very small, and an epithelial tissue is composed of many [NUMBER?] cells, so we assume that $F \to \infty$ and then immediately notice that the expression in parentheses must tend to zero as F goes to infinity, or else the left hand side of the above equation will not approach the constant 6χ So we know that the algebraic mean of the number of vertices per face must be 6. Of course we have no reason at this point to assume a distribution which guarantees that the majority of cells in the tissue will have exactly six edges and will not, say consist of a mixture of 5 and 7 sided cells. Nevertheless, empirical evidence shows a strong central tendency in the distribution of cell shapes. Whenever a cell tries to stray from the mean, there are means (such as a T3 swap, described in the next section) of recentering the distribution at 6 sides.

3.2 Why the Specified Topology Is Not Perfect

The choice to impose degree three on each vertex is not one hundred percent consistent with nature, but has been a part of most models of epithelial tissue. This is because empirical evidence shows that the *majority* of vertices in a tissue will have out degree three. It is a simplifying assumption that *rosettes* (epithelial cells organized radially about one vertex which has degree greater than or equal to 4) do not change the global dynamics of the development of an epithelial tissue. Recent computer vision developments [**?**] have made it easier to detect rosettes in epithelial tissue samples and may in the future provide information about the number of these formations, or evidence that rosettes are an important feature of epithelial tissue.

3.3 Feedback Mechanisms and Proliferation

This model is limited in that includes neither mechanical nor chemical feedback, and does not specify how cells proliferate. These are two extensions which can and have been made to the model by certain researchers. On the other hand, the dynamics of some successful models such as [**?**] have the patterning of cells specified entirely by morphogens. In these models, chemicals called 'morphogens' are what drive cells to proliferate, and the low concentrations of the morphogen on the fringe of the tissue explain why the tissue eventually ceases to grow as the tissue reaches a certain size. Other models, such as those described in [**?**] are based upon the vertex dynamics models such as the Honda-Nagai model, but include additional mechanical feedback terms which limit the growth of cells.

3.4 Additional Curiosities

The vast majority of models assume that exactly three cells meet at any vertex, except vertices on the boundary. In the language of topology, one would say that all interior vertices in the tissue have degree three. Empirical observations show, however, that more more than three cells can meet at any junction under certain circumstances [**?**]. This means that models ought to be extended to include the formation of these 'rosettes'.

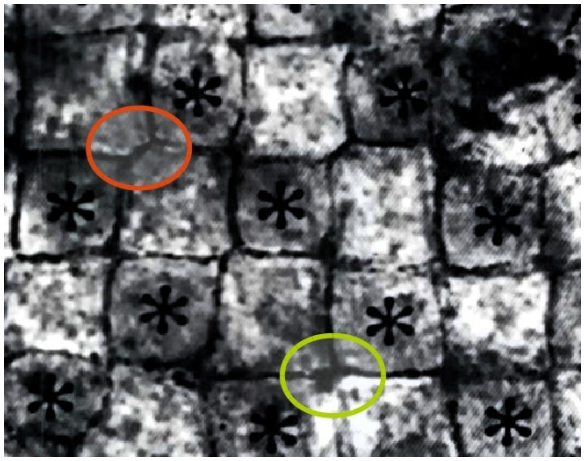

Figure 3.1: An image or Japanese quail epithelium. This tissue is patterned like a checkerboard and has been modeled in the past as a tissue with degree three vertices. It is possible that modelling this tissue as degree four vertices would provide better approximations of the dynamics. In particular, notice that the orange vertices clearly can be modeled with degree three, wherease the green vertex could be one degree four vertex or two degree three.[**?**]

Chapter 4

GrowFlesh

"All models are wrong, but some are useful" - G. Pox

4.1 About Epithelium

For my Master's Thesis I have implemented the Nagai-Honda Model for epithelial tissue development. My software is easy to install, takes up less than 50Mb, comes in parallel and non-parallel versions (Version 1.0.0, Version 1.0.1) and has very few dependencies (and they are likely already installed on mac and linux computers).

My code allows users to specify all parameters of interest in a couple of well commented configuration files, can handle simulations of arbitrarily large size, and can generate beautiful animations and plots of epithelial tissue development as well as useful plots of various quantities which are of interest to the researcher.

On top of all of this, the source code is highly modularized and allows for ambitious users to easily extend the code to meet their needs. For example, alternate numerical integrators can easily replace the existing one, new mesh generators can replace the square mesh I have developed, and all data is output in very simple formats(which users with scriting experience can transform to fit into the graphical utilities of their choice). In addition, the cell and vertex classes are well documented and can be extended to output new data, as users may need. What follow are a few graphs to give some flavor of what *Epithelium* can do.

Mention how Chaste was a step in the right direction, but the dependencies are too many and the it is difficult to get started. Epithelium is lightwiehgt and the code is easy to read, a better introductory tool.

4.2 Sample Configuration Files

4.2.1 config.txt

In this file, the user an specify some global properties about the mesh, and some important quantities for how the simulation will proceed. Most of the quantities are self explanatory. The dimension of the mesh is explained in the Code Design chapter of this paper. The swap length , upper bound, and Max Swaps parameters are used for performing random transformations to the mesh in the beginning of the simulation. The swap length is the edge length below which a swap is performed. The Max Swaps is the maximum nuber of random perturbations the code will make to the mesh. The upper bound is an integer which is upper bound of the range for a random number generator. The random swaps occur when a '1' is generated, and we choose random numbers from [1:upper bound].

OFF is the file format given to the plotting program geomview to plot the mesh. You can specify how often the code prints an image. It must be a multiple of ten, so if you want

more closely spaced images you can just drop the maximum step size for the numerical integrator. The numerical integrator takes adaptively sized steps, and this will be discussed in more detail later.

```
13 # Dimension of mesh MUST BE ODD!!!!
1 # Plot the energy in the system? [1/0]
1 # Make a movie in the end? [1/0]
0.01 # Maximum step size
1000 # Number of iterations
10 # frequency of OFF file output. Must be a multiple 10!
.1 # delta minimum vertex separation.
1000 # Max swaps
1.5 # swap length
2 # upper bound random number generator
1 # Make a bar graph of cell sides? [1/0]
0 # Make a histogram of the areas? [1/0]
0 # Make a histogram of the perimeters? [1/0]
```

4.2.2 parameters.hpp

In this header the user can define some global parameter values for the cells in the mesh. Unfortunately, you must recompile every time a parameter is changed. This could be rewritten such that parameters are read in from a configuration file, but that is just not the way the code was developed.

```
const double beta = 0.1;
const double lambda = 0.1;
const double pi = 3.141592;
const double t_gamma = 1;
const double t_area = 14.0;
```

4.2.3 changemesh.txt

This file is a configuration file, and does not require you to recompile when you change it. You can fine tune the properties of the cells in the mesh with this file.

```
# This file contains number of gamma changes,
# followed by the number of area changes,
# followed by the indices and new values
2 3
16 4.0
17 5.1
3 1.0
4 1.0
10 3.7
```

4.3 Image Gallery

This selection of graphs captures the properties of the mesh with various choices of parameter values. The target area for each cell was set to 4.0, unless otherwise specified. A couple of plots have outliers in the number of sides the cells have, or in the perimeters attained.

This is due to the individual specification of cell properties for a handful of cells. In this way, the distribution of cell properties was more finely controlled. The images come in groups of four. There are two parameter studies per page. On the right you will see the equilibrium area and perimeter reached after applying the force, and the on the right you will see the equilibrium distribution of cell shapes along with a plot of the decreasing energy in the mesh as a function of time.

Following the parameter studies several interesting tissues are presented.

4.4 Why *Epithelium* is a good piece of software

To close our discussion of *Epithelium* I would like to discuss why it is a great piece of software for *you*. *GrowFlesh* has only a couple of dependencies which are likely already installed on you computer if you are interested in computational science. You will need a compiler supporting the C++11 standard, python2.7, the matplotlib plotting library for python and the numpy python library. The only packages which will likely not be installed on your computer are the geomview geometric visualization software and the imagemagick image conversion program. Geomview and ImageMagick are free, and are such good programs that they have been around for more than 20 years. Of course, all of the animation, and plot information is outputed from this software in file formats that are easy to adapt to the user's choice of visualization software. The energy and histogram files are space separated lists and the mesh information is outputted in the OFF file format, which features a list of coordinates followed by a list of polygons which are defined counterclockwise as a list of vertex indices from the preceding list of vertices. A sample mesh file is shown below to convince you of how simple this file format is, and to suggest that you could write a smal script to change this file to a different format that will be acceptable to your choice of visualization software.

```
{appearance {+edge}
OFF
# This is the OFF formate for a square.
# We have the numVerts, numFaces, and a zero
# Then a list of vertex coordinates
# Then a list of faces described counterclockwise
# by their vertices.
4 1 0
1 0 0
1 1 0
0 1 0
0 0 0
4 1 2 3 4
```

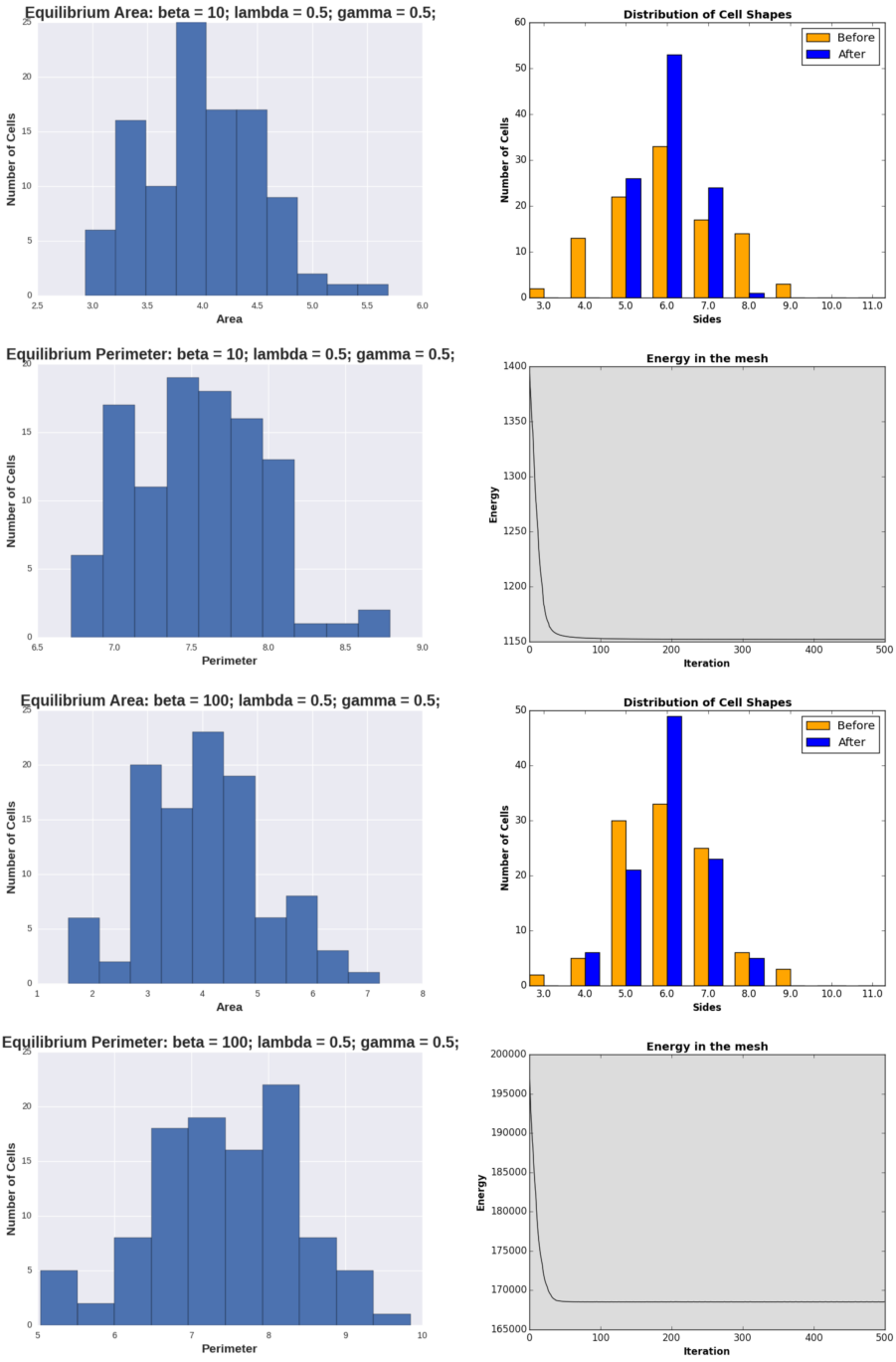

Figure 4.1: These graphs show the equilibrium reached when beta is the dominant parameter.

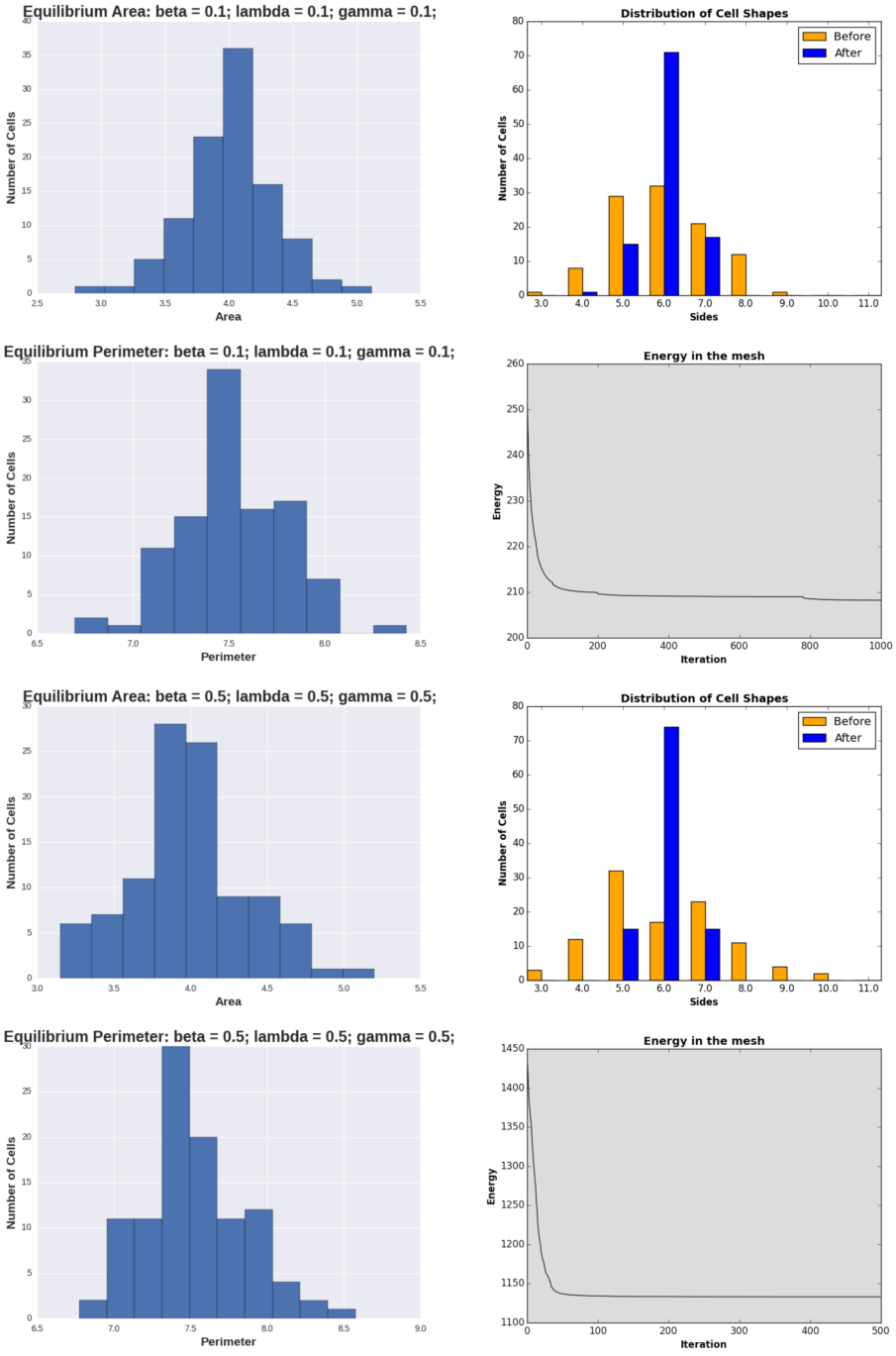

Figure 4.2: These graphs show the equilibrium reached when all parameters are set equal.

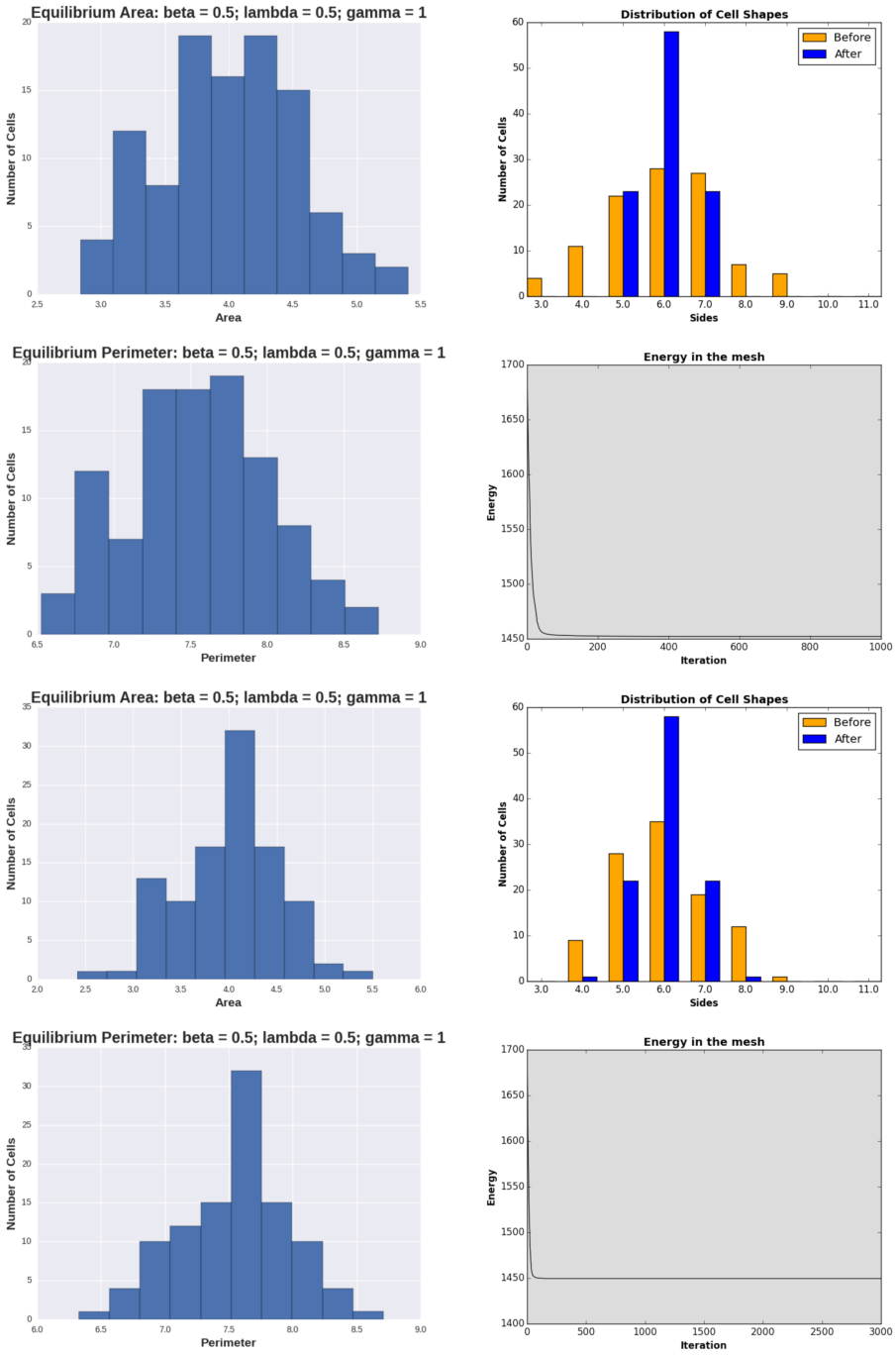

Figure 4.3: These graphs show the equilibrium reached when gamma is the dominant parameter.

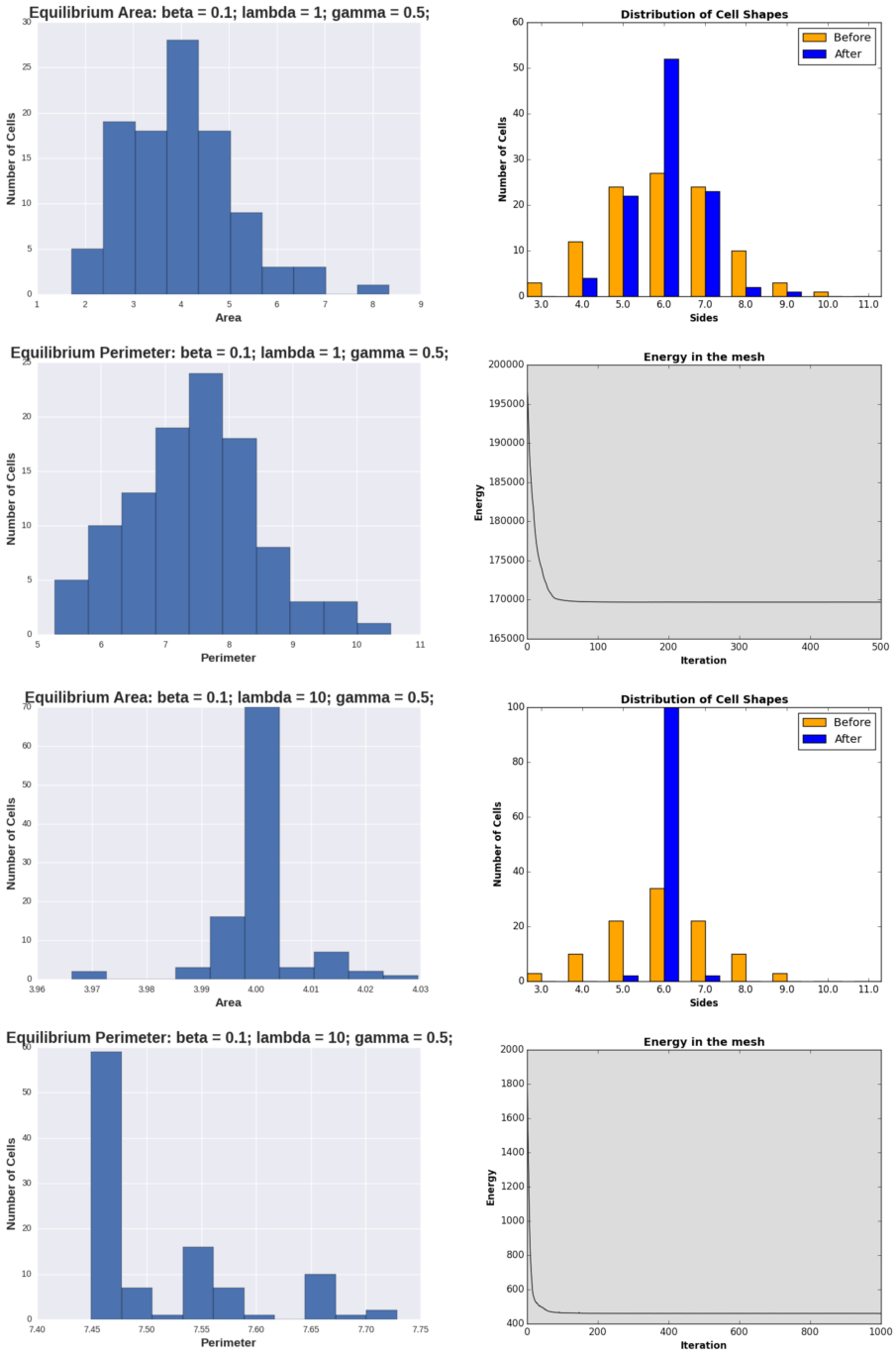

Figure 4.4: These graphs show the equilibrium reached when lambda is the dominant parameter.

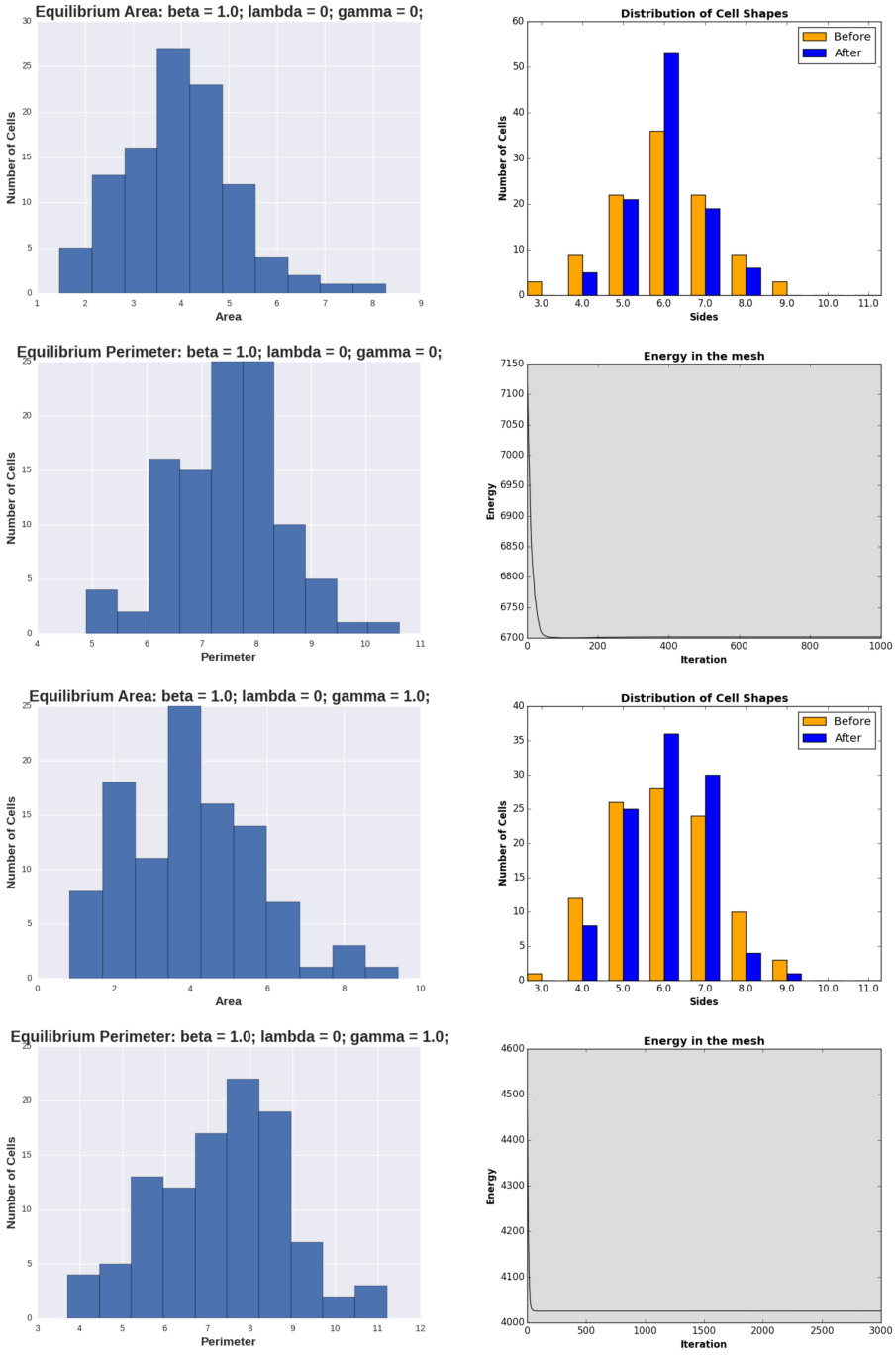

Figure 4.5: These graphs show the equlibrium in the absence of a parameter.

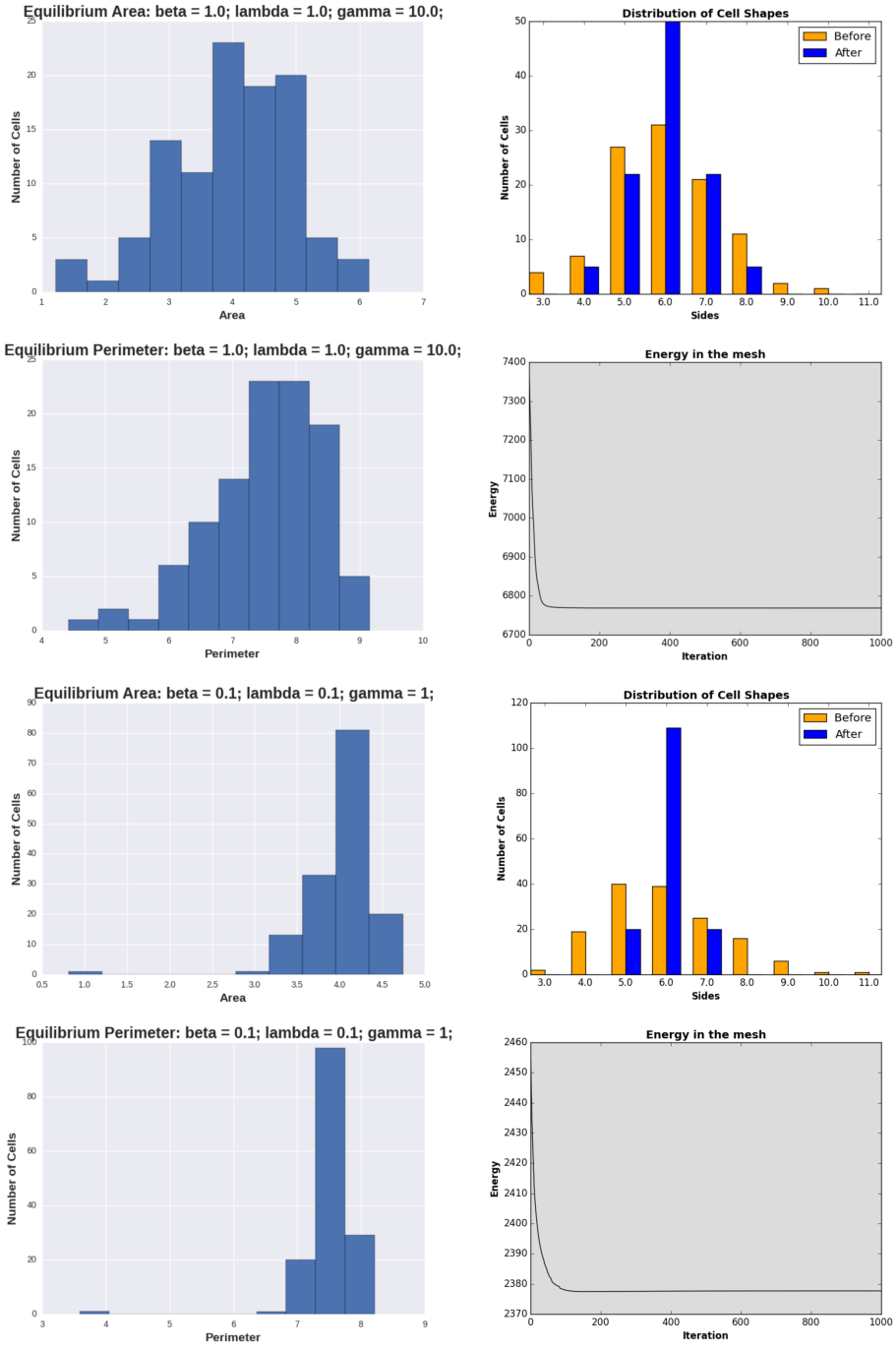

Figure 4.6: These graphs show the equilibrium reached when the target area is set to be larger than the available space in the mesh, and there is also a graph showing another gamma-dominant equilibrium.

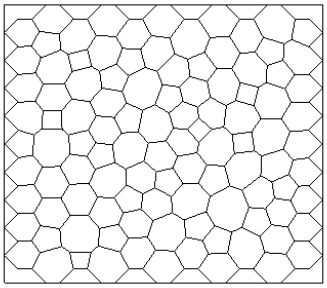

(a) A Final Mesh With White Background.

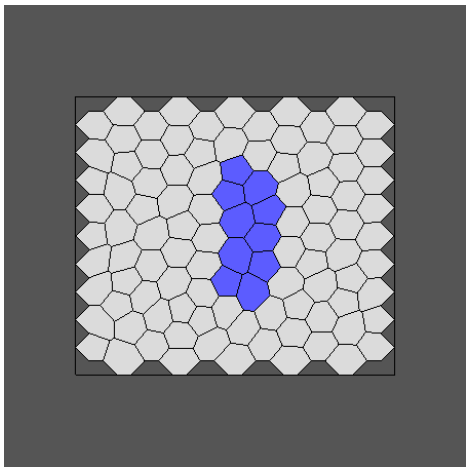

(b) A final mesh where some cells have target area < 4.0

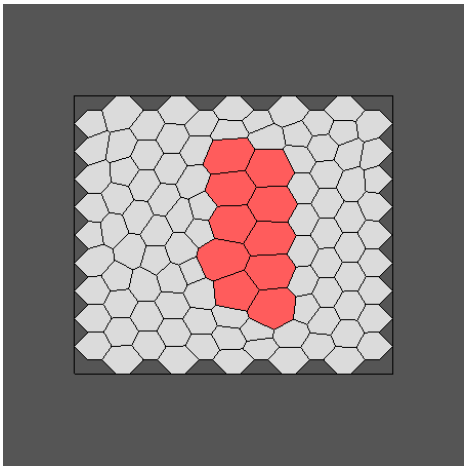

(c) A final mesh where some cells have target area > 4.0

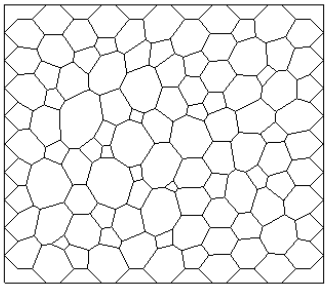

(d) A mesh during an integration, before equilibration.

Figure 4.7: A Selection of Interesting Tissues

Chapter 5

The Design of *Epithelium*

In this chapter I will explain the layout of the code, including the classes used, the data structure and the algorithms which I developed to calculate all of the inter- and intra- cellular forces governing vertex motion. A number of ideas were scrapped in the beginning of the modeling process because of the complicated relationship. The model I have implemented is a vertex dynamics model, and as such, one would think that the object of interest should be a vertex. Vertices require information about the cells which contain them in order to be moved. With this as a starting idea, I developed a sophisticated vertex class which contained cells as member variables. Apart from the software bloat coming from many vertices containing massive amounts of cell information, another issue was that cells are made of vertices, and, as such, cells out to contain vertices as member variables! Unfortunately this bilateral inclusion is not supported by C++.

5.1 [Highly Simplified] Pseudocode

5.2 Classes

Before going into how this issue was resolved in its entirely, I will describe the cell and coordinate classes.

5.2.1 The Cell Class

The cell class contains a number of useful functions and pertinent data members to make the code easy to read and understand. All cells know their index, they know which vertices make them up, they are able to calulate their area and perimeter, can modify their constituent vertices, can tell you whether or not ther contain a vertex, and can print out a graphical, color coded representation of themselves to an OFF file.

```
public:
        cell(int index, std::vector<int> AssociatedVertices,\
                double target_area = AREA, double gamma = GAMMA)
        {
                assert(index >= 0);
                m_AssociatedVertices = AssociatedVertices;
                m_index = index;
                m_target_area = target_area;
                m_target_perimeter = std::sqrt(pi * m_target_area);
                m_gamma = gamma;
        }

        cell(){}

        std::vector<int> GetVertices(){return m_AssociatedVertices;};
```

```
        int GetIndex(){return m_index;};
        void SetIndex(int index){m_index = index;};
    void SetTargetArea(double area){m_target_area = area;};
        double GetTargetArea(){return m_target_area;};
        double GetTargetPerimeter(){return m_target_perimeter;};
        double ComputeArea(double * X, double * Y);
        double ComputePerimeter(double * X, double * Y);
        void PrintCell(std::ofstream &OffFile);
        int ContainsVertex(int index);
        void SetGamma(double gamma){m_gamma = gamma;};
        double GetGamma(){return m_gamma;};
        void InsertVert(int v1, int v2);
        void EraseVert(int index)
        {
                std::vector<int>::iterator it = std::find(m_AssociatedVertices.begin
                        m_AssociatedVertices.end(), index);
                m_AssociatedVertices.erase(it);
        };
        void ReplaceVert(int before, int after)
        {
                std::vector<int>::iterator it = std::find(m_AssociatedVertices.begin
                        , m_AssociatedVertices.end(), before);
                *it = after;
        };
        void SetVertices(std::vector<int> vertices){m_AssociatedVertices = vertices;
        int GetNumSides(){return m_AssociatedVertices.size();};
private:
        std::vector<int> m_AssociatedVertices; //Counterclockwise
        int m_index;
        double m_target_area;
        double m_target_perimeter;
        double m_gamma; // We can change this later.
};
```

5.2.2 The Coordinate Class

The coordinate class stores the index of a coordinate, and whether or not the vertex will move during the integration. My code will run with two types of meshes: meshes with border, and meshes without. A mesh with border is a mesh with fixed border elements. A mesh without border is a mesh which was generated with periodic boundary conditions and which maintains the periodicity throughout the calculations done by the program. Border vertices will not move, whereas interior vertices will be able to move; the coordinate class allows us to secify whether or not a vertex is interior or exterior. Another benefit of this class is that is allows use to easily extend the code to include forces acting on individual vertices, and to specify other types of vertices besides interior and exterior. This code was developed with eyes to the future.

```
class coordinate
{
public:
        coordinate(int idx, bool t) : index(idx), IsInner(t){};
        coordinate(){index = -1; IsInner = 0;};
```

```
        int index;
        bool IsInner;
        inline bool operator==(const coordinate& rhs){return index == rhs.index;};
};
```

5.3 Initial Mesh Design

5.4 A Relational Database

A popular way to store data since the 1970's is to store data in group of tables which are connected via *keys*. This database is popular in business for reasons which will become apparent by means of a simple example.

Consider a business which sells a number of products, and wants to keep track of their customers, the customers orders, the customers addresses, and information about the products ordered. A wasteful way to store this data is to store a large table with a column for customer. Next to every customer's name is the customers address. Next to the customers address is the customer's order number. Next to the customer's order number is a column of items ordered. And, next to each item ordered is the item information. This method of storing data is terribly redundant, because for every customer's order which contains item X, the description of item X is stored in the table next to X. Furthermore, one customer may make several orders, so the customer's information will be stored multiple times for each order number.

A better idea is to break this data up into several tables which together define a *schema* for the data. In one table we store customer and customer infromation. In the second table we store a list of order numbers, and for each order number a set of identifying tags for the products ordered. Then, in another table we store the company's inventory as a table in which item information can be accessed via the tag stored in the order table. Now we have three nonredundant tables from which information can be extracted via *join* operations. A join operation extracts the rows from two tables which contain matching keys.

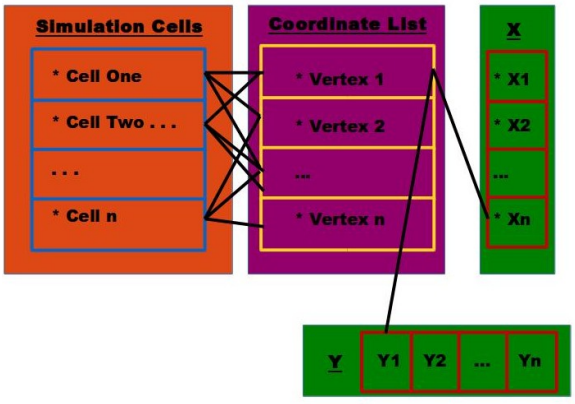

Figure 5.1: The Relational Database

The code I have written implements this relational database model. I have six tables, including the simulationCells, coordinateList, X, Y, tempX and tempY tables. The cell and coordinate tables are implemented as 1d vectors of cell and coordinate objects, whereas the

position tables are implemented as 1d arrays for ease of passing these structures to Cuda C functions which will speed up the computation. We will talk more about Cuda C and the parallelization of this code in a later section. The cells can extract coordinate information from the coordinateList table via the *index* key, and the coordinateList can access the position information from the X and Y arrays via their own *index*. The temporary X and Y arrays store temporary position information about the vertices before the mesh positions are updated. My algorithm is a fault tolerant algorithm in that in checks for computational flaws in the temporary location arrays before updating the actual X and Y arrays, which would invalidate the entire computation.

5.5 Moving the Vertices

Version 1.0.0, the latest stable release of*Epithelium* loops over the vertices in the mesh and, for each one, computes the force applied to each vertex and then computes a displacement due to the force using the Euler Method. In their original paper, H. Honda and T. Nagai described the use of a Modified Runge Kutta Method to move the vertices, but this method would result in extra unnecessary computations at each time step. For our purposes we only need the precision offered by the Euler Method because our model is a qualitative model, not a quantitive model, and does not require the accuracy of more complicated method. So long as the parameters in the code do not have physical significance, there is no need to worry about rounding errors in our code. This was the decision made by the research group at Oxford that developed CHASTE, the *other* leading software for implementing the Nagai-Honda Model.

For now, a displacement is calculated and stored in a temporary X vector. No vertex is permitted to move more than one half of the minimum delta separating vertices (the δ under which a T1 swap will occur). In this way we can guarantee two things: 1)We will never miss the occurence of two vertices coming critically close to each other for a T1 swap and 2) If a vertex were allowed to move more than this distance, it is possible that two vertices located at a distance of slightly over δ might move past each other and invalidate the mesh. For our adaptive time stepping, the integration starts with a user defined maximum time step and begins to loop over all of the vertices in the mesh. The results of the integration are stored in the temporary X array. If the vertex happens to have moved too much, then the entire set of integrations for that time step is invalidated, the time step is halved, and the procedure starts over.

Another important aspect of the numerical integration is that information about the cells which contain the vertex must be processed in a counter clockwise order, as previously discussed. For example, when performing the force calculation for the force which comes from the area term, we need to retrieve the areas of the involved cells in counterclockwise order. We do this by finding the finding the next vertex in the current cell, which is stored in the vertex array of the cell in counterclockwise order. Now we look for that vertex and the current vertex in some other cell in the mesh. We know that that cell must be clockwise from the current cell. See Figure **??**.

5.6 Embarassing Parallelism and CUDA

The numerical integrations and the updating vertex locations steps of the code exhibit what MATLAB co-founder Cleve Moler describes as “embarassing parallelism”. Computing the

displacement of vertex a does not depend upon the computation of the displacement of vertex b during a given time step. Similarly, the vertex locations can all be updated in parallel since the update is simply a vector sum operation of the X and Y arrays with the temporary X and Y arrays, respectively. CUDA was also employed in *GrowFlesh* to rotate the mesh through a parallelized matrix multiplication, and to find the maximal absolute difference in the rotated X and not rotated X arrays using a common parallel reduction technique.

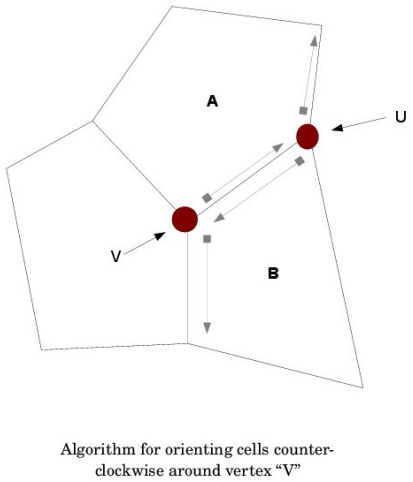

Figure 5.2: Getting Cells in Order

A popular hardware choice for parallel programming in last decade has been the NVIDIA GPU. Thanks to the generous support of the Sotomayor Lab at Ohio State where this paper and software have been written, I was able to work on a computer which has a very powerful CUDA capable GPU. CUDA is the NVIDIA extension of the C programming language which can specifiy which part of a piece of code to run on the CPU, and which parts to run on the GPU. The CUDA capable GPU features many simple microprocessors which can perform only rudimentary arithmetic operations. This is an ideal piece of hardware for a piece of code which has to perform many arithmetic operations which do not have inhibiting data dependencies.

INSERT IMAGE of a CUDA CPU ALONGSIDE SOME ARRAYS TO MAKE IT CLEAR HOW THIS HAPPENS

So far, I have not written the force vector calculations in CUDA since CUDA essentially operates on C arrays, and most cell data is stored in C++ vector of various sizes.

5.7 Computing Topological changes.

The algorithm for performing a T1 swap goes as follows:

5.7.1 Eight Cases For Coordinate Placement in a T1 Swap

1. **Given:**
   I.x ¡ Ip1.x AND I.y == Ip1.y **Then:**
   I $\mapsto$ mp + (0, -dy) AND Ip1 $\mapsto$ mp + (0, dy)

2. **Given:**
   I.x ¿ Ip1.x AND I.y == Ip1.y **Then:**
   I $\mapsto$ mp + (0, dy) AND Ip1 $\mapsto$ mp + (0, -dy)

3. **Given:**
   I.x ¡ Ip1.x AND I.y ¡ Ip1.y **Then:**
   I $\mapsto$ mp + (dx, -dy) AND Ip1 $\mapsto$ mp + (-dx, dy)

4. **Given:**
   I.x ¿ Ip1.x AND I.y ¿ Ip1.y **Then:**

I $\mapsto$ mp + (-dx, dy) AND Ip1 $\mapsto$ mp + (dx, -dy)

5. **Given:**
   I.x ¡ Ip1.x AND I.y ¿ Ip1.y **Then:**
   I $\mapsto$ mp + (-dx, -dy) AND Ip1 $\mapsto$ mp + (dx, dy)

6. **Given:**
   I.x ¿ Ip1.x AND I.y ¡ Ip1.y **Then:**
   I $\mapsto$ mp + (dx, dy) AND Ip1 $\mapsto$ mp + (-dx, -dy)

7. **Given:**
   I.x == Ip1.x AND I.y ¿ Ip1.y **Then:**
   I $\mapsto$ mp + (dx, -dy) AND Ip1 $\mapsto$ mp + (-dx, dy)

8. **Given:**
   I.x == Ip1.x AND I.y ¡ Ip1.y **Then:**
   I $\mapsto$ mp + (dx, -dy) AND Ip1 $\mapsto$ mp + (-dx, dy)

5.7.2 The implementation of the T2 swap.

5.8 Error Tolerance of the Algorithm

GrowFlesh has been empirically shown to be numerically stable and the code outputs an error measurement at the end of a simulation to give the user a sense of the accuracy of the preceding computation. So, while there is no analytical proof of stability we always have a measure of stability to help us aid our confidence in the code. *GrowFlesh* runs two simultions at the same time, one on the mesh described above, and another on the same mesh which has been rotated 45 degrees. The, at the end of a simulation the rotated mesh is rotated back and corresponding vertices are compared by index using the Euclidean norm to decide whether the rotation of the coordinates induced any change in the dynamics of the simulation due to floating point round off.

CUDA was used to multiply each vertex in the mesh by the rotation matrix:

$$\begin{pmatrix} \cos\theta & -\sin\theta \\ \sin\theta & \cos\theta \end{pmatrix}$$

5.9 The C++ Standard Library, and Use of the New Library.

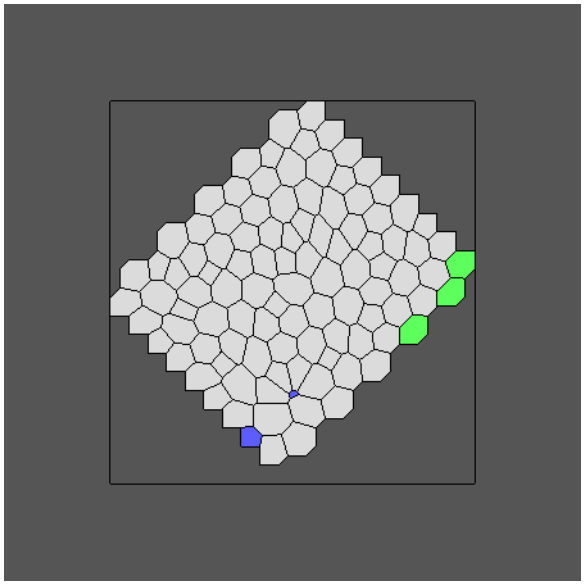

Figure 5.3: A Rotated Mesh for Error Analysis.

Bibliography

[1] K. Bambardekar et. al. Direct Laser Manipulation Reveals the Mechanics of Cell Contacts In Vivo *PNAS* **112** 1416-1421.

[2] Buchmann, A. Alber, M., Zartman, J. *Sizing it up: The mechanical feedback hypothesis of organ growth regulation.* Seminars in Cell and Developmental Biology, 2014.

[3] *Chaste Tutorial* `https://chaste.cs.ox.ac.uk/chaste/tutorials/release_2.1/UserTutorials.html`

[4] Drasdo, D. *Bucking Instabilities of One Layered Growing Tissues.* Physical Review Letters 84.

[5] Durand, M., Stone, H. Relaxation Time of the Topological T1 process in a Two Dimensional Foam. arXiv.0

[6] *Epithelial Tissues* `http://www.botany.uwc.ac.za/sci_ed/grade10/mammal/epithelial.htm`

[7] Farhadifar, R., Roper, J., Algouy, B., Eaton, S., Jullcher, F. The Influence of Cell Mechanics, Cell-Cell Interactions, and Proliferation on Epithelial Packing. *Current Biology* **17** 2095-2104. (2007)

[8] Fletcher, A. , Osterfield, M., Baker, R., Shvartsman, S. *Vertex Models of Epithelial Morphogenesis.* Biophysical Journal 106, June 2014.

[9] Fletcher, A., Osborne, J., Maini, P, Gavaghan, D. *Implementing vertex dynamics models of cell populations in biology within a consitent computational framework.* Prog. Biophys. Mol. Biol. 113: 299 - 326.

[10] Gibson, W., Gibson, M. *Cell Topology, Geometry, and Morphogenesis in Proliferating Epithelia.* Current Topics in Developmental Biology **89** 87-114. (2009)

[11] T. Gillies and C. Cabernard. Cell Division and Orientation in Animals. *Current Biology* **21** 599-609

[12] P. Grassia, C. Oguey, R. Saepitomi. Relaxation of the topological T1 process in a two-dimensional foam. *The European Physical Journal E* **35** (2012)

[13] H. Honda. Description of Cellular Patterns by Dirichlet Domains: The Two-Dimensional Case. *Journal of Theoretical Biology* **72** 523-543. (1978)

[14] H. Honda, H. Yamanaka, M. Dan-Sohkawa. A Computer Simulation of Geometrical Configurations During Cell Division. *Journal of Theoretical Biology* **106** 423-435. (1984)

[15] Honda, H. Essence of Shape Formation in Animals. *Forma*, **27** S1-S8. (2012)

[16] K. Kawasaki, T. Nagai, K. Nakashima. Vertex models for two-dimensional grain growth. *Philisophical Magazine Part B* **60** 399 - 421. (1989)

[17] K. Liu, S. Ernst, V. Lecaudey, O. Ronneberger. Epithelial Rosette Detection in Microscopic Images.

[18] Luebke, D. and Owens, J. *Intro to Parallel Programming* `https://www.udacity.com/course/cs344` 2013.

[19] Marshall et. al. What Determines Cell Size? *BMC Biology* **10** (2012)

[20] T. Nagai and H. Honda. Wound Healing Mechanism in Epithelial Tissues Cell Adhesion to Basal Lamina. *Proceedings of the 2006 WSEAS Int. Conf. on Cellular & Molecular Biology, Biophysics & Bioengineering***2006** (pp111-116)

[21] Nagai, T. Honda, H. A dynamic model for the formation of epithelial tissues. *Philisophical Magazine, Pt. B.***81**(2001)

[22] R. Nagpal, A. Patel, M. Gibson. Epithelial Topology. *BioEssays* **30** 260-266. (2008)

[23] K. Nakashima, T. Nagai, K. Kawasaki. Scaling Behavior of Two-Dimensional Domain Growth: Computer Simulation of Vertex Models. *Journal of Statistical Physics* **57** 759-787. (1989)

[24] Ohlenbusch, H.M., Aste, T. Dubertret, B., Rivier, N. The Topological Structure of 2D Disordered Cellular Structures. arXiv.

[25] S.Okuda et. al. Reversible Network Reconnection Model for Simulating Large Deformation in Dynamic Tissue Morphogenesis. *Biomech Model Mechanobiol* **12** 627-644 (2013)

[26] `http://www.millerplace.k12.ny.us/webpages/lmiller/photos/636532/Epithelial\%20TissueTypes.bmp`

[27] Potential Energy Graph `http://images.tutorvista.com/content/work-energy-power/potential-energy-variation.gif`

[28] K. Ragkousi and M. Gibson. Cell Division and the Maintenance of Epithelial Order. *Journal of Cell Biology* **207** 181-188

[29] Restrepo, S., Zartman, J. , and Basler, K. *Coordination of Patterning and Growth by the Morphogen DPP* Current Biology 24, 245- 255

[30] R. Thom. Topological Models in Biology. *Topology* **8** 313- 315 (1969)

[31] Weaire, D. and Rivier, N. *Soap, Cells, and Statistics*

[32] H. Yamanaka and H. Honda. A checkerboard pattern manifested by the oviduct epithelium of the Japanese Quail. *Int. J. Dev. Biol.* **34** 377-383.

Appendix A

Valuable Programming Lessons Learned

A.1 GitHub

When you are working on a large project such as this one, it is a good idea to have some sort of version control system which tracks the changes you have made to your code, and to return to an earlier working version in case something gets terrribly broken. Many people who do not know about version control will do just this, except they will save as' every couple of days. Unfortunately, this method is very space inefficient, as each time you 'save as', you save your entire project. Roughly speaking, git saves only the small changes you have made between versions. Git is a popular version control tool, and github is a popular place to store you files online.

Get Your Files on GitHub

- Go to github.com and sign up for an account
- Make a new repo on github
- cd to the directory of your project on your machine.
- git init
- git add .
- git commit -m "some message"
- git remote add origin YOUR URL HERE (This url is given to you from github when you make the repo.)
- git pull origin master
- git push origin master

Access And Modify These Files Somewhere Else

- Simply type git clone `urlofrepositoryhere` into a terminal
- Work on project
- git push origin master, when done working.

Appendix B

How Several Programming Languages Were Used In Harmony